The Relationship of the Change in Hydrogeochemical Features and Lithium Values of Kızılırmak Basin (Nevsehir-Central Anatolia) Water with Tectonic Fields

Ramazan DEMİRCİOĞLU[1]* and Hatim ELHATİP[2]

Authors' affiliations and addresses:
[1]Department of Emergency Aid and Disaster Management, Aksaray University, Aksaray 68100, Turkey
e-mail: ra.demircioglu@gmail.com

[2]Department of Environmental Engineering, Aksaray University, Aksaray 68100, Turkey.
e-mail: helhatip@gmail.com

*Correspondence:
Ramazan Demircioğlu, [1]Department of Emergency Aid and Disaster Management, Aksaray University, Aksaray 68100, Turkey
tel.: +905425979432
e-mail: ra.demircioglu@gmail.com

Abstract
In this study, in particular, the relationship between high lithium values and geological environments was examined. To determine this, the geology, structural geology, hydrogeology, and hydrogeochemistry of the area in the north of the Gülşehir-Yeşilöz sub-basin of the Kızılırmak Basin were investigated. For hydrogeological studies, 19 water samples were collected in May and September. Tectonically, this area has a horst-graben structure. The relationships between the water analysis values of the study area and the tectonic areas were investigated. In particular, the lithium content of the waters in the study area was investigated. Hydrogeochemical properties and seasonal changes in water resources were studied in detail, and their relationship with tectonic areas was evaluated. Water analyses were carried out during wet and dry periods to determine temporal hydrogeochemical changes. According to the analysis, the waters in the area are of Ca-HCO$_3$ and Ca-Mg-HCO$_3$ facies. In addition, there are water samples with high lithium content in the study area. IDW and Kernel diagrams of these were prepared. It was found that these high values were influenced by the rocks formed in the ancient sea and saline lake environments. The region with the highest lithium value is in the formations that represent the former salt lake environment. High lithium (Li) values are generally higher in the region within the Kızılırmak graben. Lithium values in this area were determined as 241.3 µg/L, 154.5 µg/L, 155.2 µg/L, 156.8 µg/L, and 155.6 µg/L.

Keywords: Hydrogeology, water analyses, salt lake, lithium.

Introduction

Lithium has become increasingly important in recent years, especially in the energy sector. It is used as an electrode material in batteries and plays a crucial role in portable devices and electrical power supplies. Lithium batteries have become more popular than other types due to their high energy density, lightweight, and long life. Research into extracting lithium from salty waters has intensified, as it is particularly abundant in these waters. Many studies have been conducted on lithium in recent years, including Belova (2017), Kavanagh et al. (2017), Liu and Agusdinata (2020), Kaunda (2020), Sulistiyono et al. (2022), and Ighalo et al. (2022). Huang and Wang (2018), Huang and Wang (2019), Zante et al. (2019), Wang et al. (2020), Zhang et al. (2021), and Kim et al. (2021) are some of the studies investigating lithium extraction from salty waters with developing technology.

The study area is located in the surroundings of the Avanos-Gülşehir districts, situated in the north of Nevşehir, in the Central Anatolian region (Fig. 1). To carry out this study, geological, structural, and hydrogeological maps at a scale of 1:25.000 were prepared for the area.
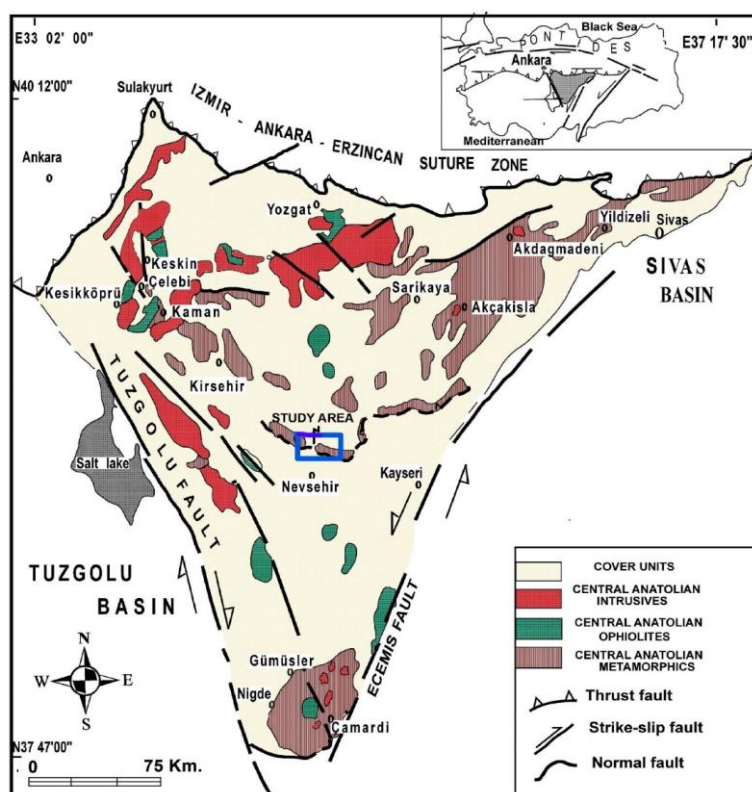

Fig. 1. Study area and location map (Modified from Kuşçu, 2001).

This study aims to investigate the high lithium values in the study area, especially in waters with high salinity. Studies have shown significant relationships between lithium and salt lakes, including those by Godfrey and Álvarez-Amado (2020), Li et al. (2021), and Li et al. (2023).

The study area is geologically located in the central part of the Kırşehir massif. Several geological studies have been conducted in the area, including stratigraphic-tectonic studies by Seymen (1982) in the north of the study area and stratigraphic studies by Atabey et al. (1988) in the south. Other geological studies include petrographic studies by Batum (1978), Aydın (1984), Ercan et al. (1991), Göncüoğlu (1993), and Köksal and Göncüoğlu (1997), and tectonic feature studies by Doğan et al. (2009), and Demircioğlu (2014).

Hydrogeological studies in the study area include Demircioğlu (2021), and Özdemir et al. (2022). This study also aims to determine whether the high lithium content detected in the waters of the area can be extracted.

This situation may require a detailed study. There is no previous study on this subject in the field. It is also a new study on the relationship between geodynamic evolution and lithium. In this study, this relationship was determined.

Another important aspect of this study is determining the rocks that show aquifer properties in and around the study area to determine the groundwater potential and the hydrological flow directions of the groundwater. Finally, the hydrogeological properties of surface and groundwater were investigated.

Geologıcal Background

The study area is located within the Central Anatolian Massif of the Anatolian Belt according to the classification of Turkey's tectonic units by Ketin (1966). Pontides form the northern part of the study area and are separated from other tectonic units by the İzmir-Ankara-Erzincan suture zone. The study area is almost in the centre of the Central Anatolian Massif. According to Okay and Tüysüz (1999), the area is bounded by the Inner Taurus suture in the east and southeast and the Ankara-Erzincan zone in the north (Fig. 1). The region and its surroundings are therefore very rich in igneous rocks, called the Cappadocian Volcanic Region. Much petrographic research has been done in the region. Studies have been carried out on the depth and surface magmatism in the area (Atabey 1988; Aydar 2012). The studies carried out have tried to show the existence of magmatism at different time intervals in the area. The Cenozoic volcanic activity in the area, which gives an age between the Late Miocene and Quaternary, is also closely related to the neotectonic structural elements in the region (Fig. 2). During this period, crustal thinning and faulting caused by the extensional tectonic regime led to reduced mantle pressure and volcanic eruptions in weak fault zones, and analyses of igneous rocks here show many volcanic activities from Late Cretaceous to Quaternary.

Geology of the study area

Metamorphic rocks belonging to the Kırşehir Massif form the basis of the study area. These units are cut by Late Cretaceous igneous rocks. These basic units are unconformably overlain by marine Palaeocene-Eocene sedimentary rocks (Figure 2). These units are unconformably overlain by Middle Miocene-Pliocene units. All these units are unconformably overlain by Quaternary alluvium.

Tectonic features of the study area were also investigated. The stratigraphic and tectonic features of the area were determined by detailed studies (Demircioğlu, 2014). The study area is located in the region called Kırşehir Massif, which is in the middle of the Central Anatolian massif. It shows that the rocks in this area were under the influence of at least 2 orogenic activities. The folds formed as a result of polyphase deformation observed in the rocks belonging to the Kırşehir Massif in the basement indicate that the rocks belonging to the massif were affected by the Kimmeridian orogenesis and the subsequent Alpine orogenesis.
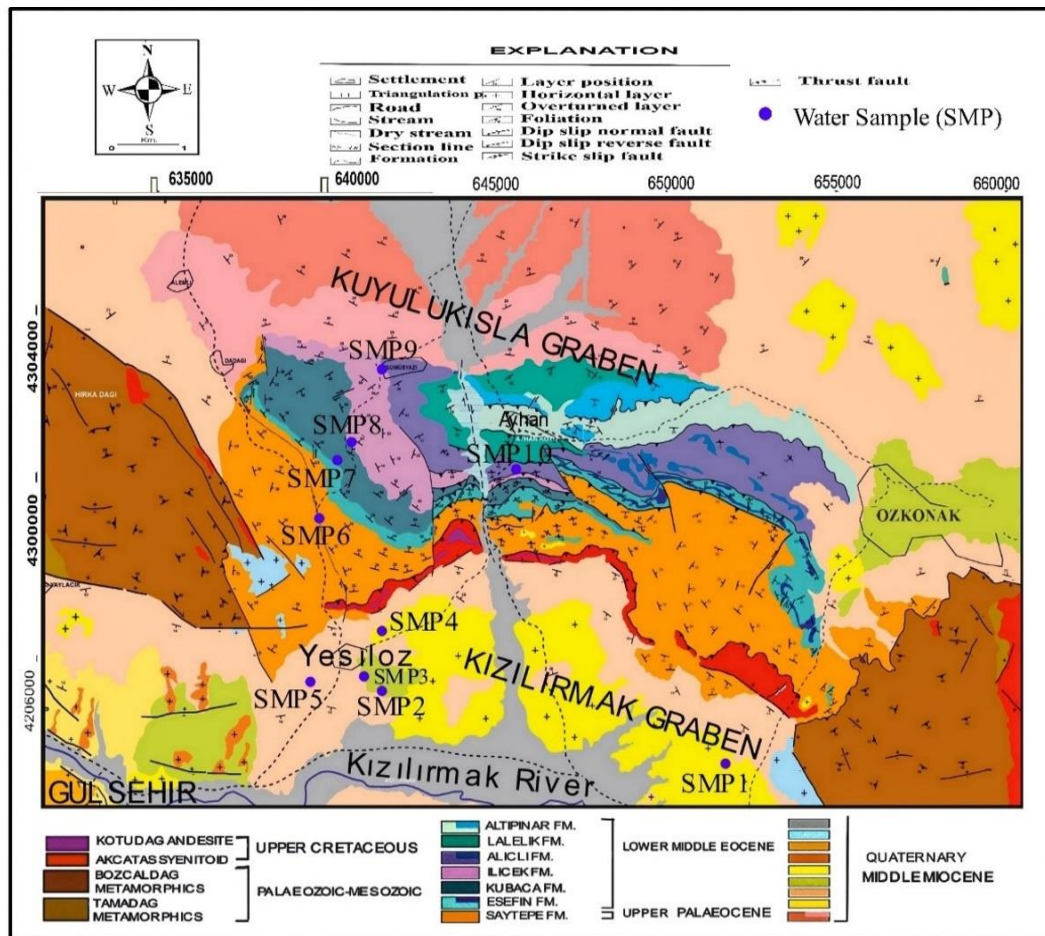

Fig. 2. Geological map of the study area (modified from Demircioğlu, 2014).

Palaeocene-Eocene units underwent folding and faulting. These units underwent three phases of folding and faulting under the post-Eocene and pre-Middle Miocene compressional tectonic regimes (Figure 3). The Ayhan shear zone was formed in this area with thrust structures and various fold types Demircioğlu and Eren, (2021). The area called the Ayhan shear zone is the area where imbricate thrust faults are located (Fig. 3). In this area, the density of strike-slip and thrust faults due to the compression tectonic regime is remarkable. These faults are observed in the Late Palaeocene-Middle Eocene rocks of the Ayhan group. Fault density is lower in younger units because they are less deformed. Directional and strike-slip fault types can be observed in the study area. Faults are present in all rock types of the massif in all directions. These faults are the result of polyphase deformation.

During the Late Miocene (Messinian)-Pliocene period, normal faulting generally occurred since the region was dominated by an extensional tectonic regime. Normal faults (Salanda, Dadağı faults) developed during this period formed the Hırka and Ziyarettepe horsts. Kuyulukisla and Kızılırmak grabens were formed between these horsts (Demircioğlu, 2014). The study area is structurally located between the Kızılırmak graben and Ziyarettepe horst. The extensional tectonic regime of the region continues today.

The rocks, which have undergone polyphase deformation, have gained a faulted and fractured structure. These fractured and fractured structures have given the rocks aquifer properties.
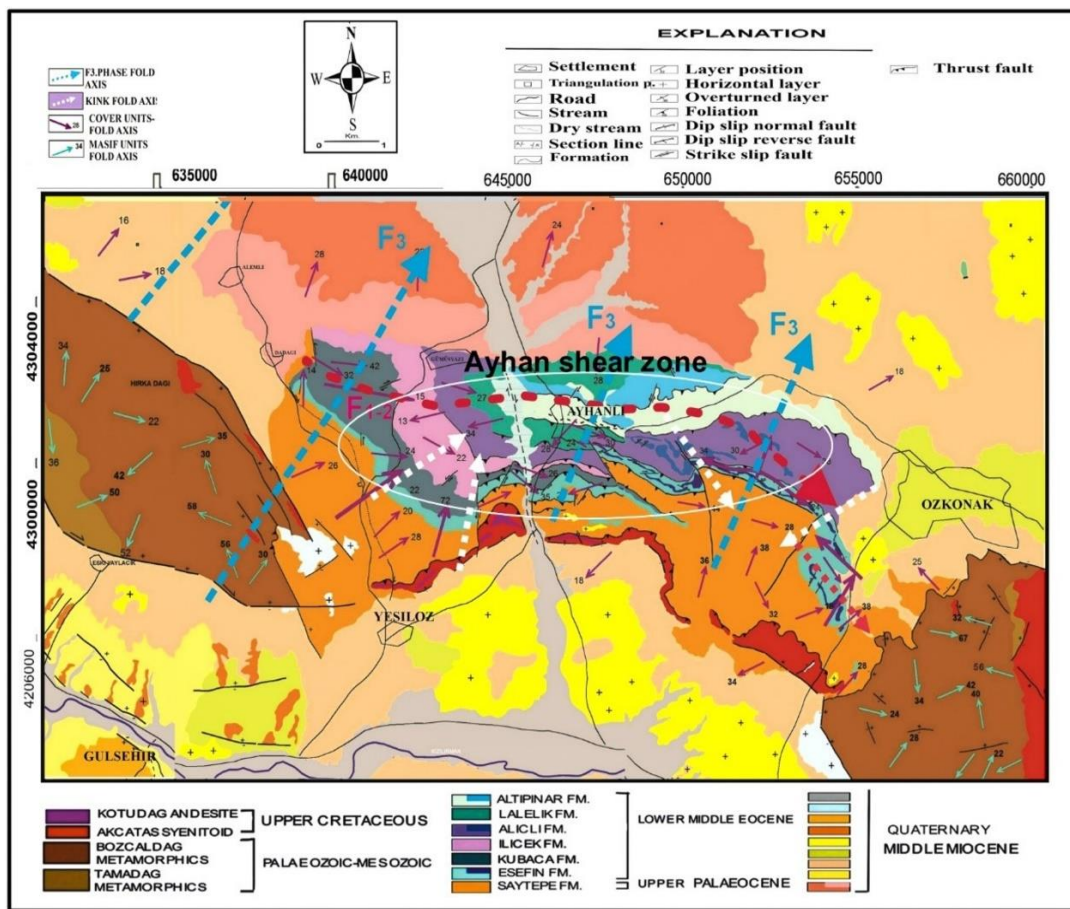

Fig. 3. Structural map of the study area (modified after Demircioğlu, 2014).

Material and Methods

The study area is the region surrounding the Avanos-Gülşehir districts, located north of Nevşehir in the Central Anatolian region. To understand the geology, structure, and hydrogeology of the area, maps were prepared at a scale of 1:25.000. The hydrogeological characteristics of the formations in the area were also considered, and water samples were collected from 10 springs in May 2019 and 9 springs in September 2019. Water samples were taken in May to represent the wet period and in September to represent the dry period. Unfortunately, one of the springs (SMP1) had dried up by September. On-site measurements of pH, temperature (T), and electrical conductivity (EC) were taken using an ISOLAB portable meter. The chemical properties of the water samples were determined in 1-litre polyethene containers to avoid altering the chemical composition of the water. Anionic (Ca^{+2}, Mg^{+2}, Na^+, K^+) and cationic (HCO_3^-, CO_3^-, SO_4^{-2}, Cl^-) analyses of the groundwater were carried out in the laboratory. The ICP-OES (Inductively Coupled Plasma-Optical Emission

Spectrometer) method was used for cation and trace element parameters, and the IC (Ion Chromatography) method for anion parameters. The collected water samples were analyzed at Aksaray University's Department of Environmental Engineering Laboratories and Water Chemistry Laboratory, which has national accreditation (Turkish Accreditation Institution-Türkak). The results of the analyses are presented in tables (Table 1, 2, 3, 4, 5). Piper, IDW, and kernel plots were used to evaluate the values obtained. IDW and Kernel plots were prepared to estimate the distribution values of lithium.

Results and Discussion
Hydrogeological Characterıstics of The Study Area

This section describes the hydrogeological characteristics, types, and locations of the water resources of the geological units in the study area and its surroundings. All waters in the study area are $Ca-(HCO_3)_2$-facies waters with high carbonate alkalinity and hardness. The fact that these waters are $Ca-(HCO_3)_2$ facies indicates that they are fed by a carbonate aquifer. The clustering of waters in the same region on the Piper diagram indicates that they are fed by the same source or a similar aquifer. When the analysis results of the samples collected in September are examined on the Piper diagram, the Mg contents of samples SMP6, SMP7, SMP8, SMP9, and SMP10 taken from the region within the Ayhan slip zone have increased. These waters are carbonate and dolomitic waters with high carbonate alkalinity and $Ca-Mg(HCO_3)_2$ waters with high hardness. The fact that these waters are $Ca-Mg-HCO_3$ facies indicates that they are fed by a carbonate aquifer with high dolomite content. The clustering of waters in the same region on the Piper diagram may indicate that they are fed by a related aquifer. Higher $Ca-Mg (HCO_3^-)_2$ facies are observed in the northern part (Ayhan shear zone), where tectonic structures are abundant. The high lithium content observed in some of the water samples in the area varies according to the tectonic areas. The IDW and core diagrams also show the relationship between the tectonic areas and stratigraphic units. Lithium ratios are high in units formed in old salty lake environments. Lithium ratios are high in units formed in ancient saline lake environments. In the study area, a 1/25.000 scale geological and water sampling map of the study area, belonging to the K33a3 map of Turkey, was prepared by field studies (Figure 2). The aquifer units in the study area are Bozçaldağ Metamorphics, marbles and coarse-grained pebbles, red-purple pebbles, and sandstones, which are highly jointed and fractured as a result of tectonism.

There are permeable and impermeable units in the study area. The karstic, jointed, and fractured sections of the metamorphic and marble rocks of the Kırşehir Massif, which form the basis of the units in the area, are permeable. Shale and clayey units are impermeable. Granites and syenites among igneous rocks are generally impermeable, but altered and highly fractured upper parts are permeable. Loosely cemented limestones, conglomerates, and sandstones of Quaternary units formed in terrestrial environments in the study area are permeable, siltstones are semi-permeable, and claystones are impermeable. Basalts and andesites formed as a result of volcanism are permeable in cooling and tectonically connected sections. However, tuff, tuffite, and volcanic ashes are generally impermeable. Secondary permeability is present in faulted and fractured rocks. The recharge system of the aquifers in the study area is generally caused by precipitation coming from the high regions, i.e. from the feeding areas. Data on irrigation wells in the region were obtained from the DSI Kayseri Regional Directorate to determine the groundwater mobility in the region. Using the ArcMap application of ArcGIS software, a groundwater level map of the region was prepared, and the groundwater flow direction was determined (Figure 4a). A drainage network map was prepared using the ArcMap application of ArcGIS software (Figure 4b).

According to these maps, although groundwater flows in different directions, a general flow can be observed towards the Kızılırmak River in the south. Based on these data, it is determined that the groundwater feeds the Kızılırmak River. In addition, the study area is divided into two sub-basins in the drainage network map (Figure 4b). This is due to changes in the geomorphological structure.
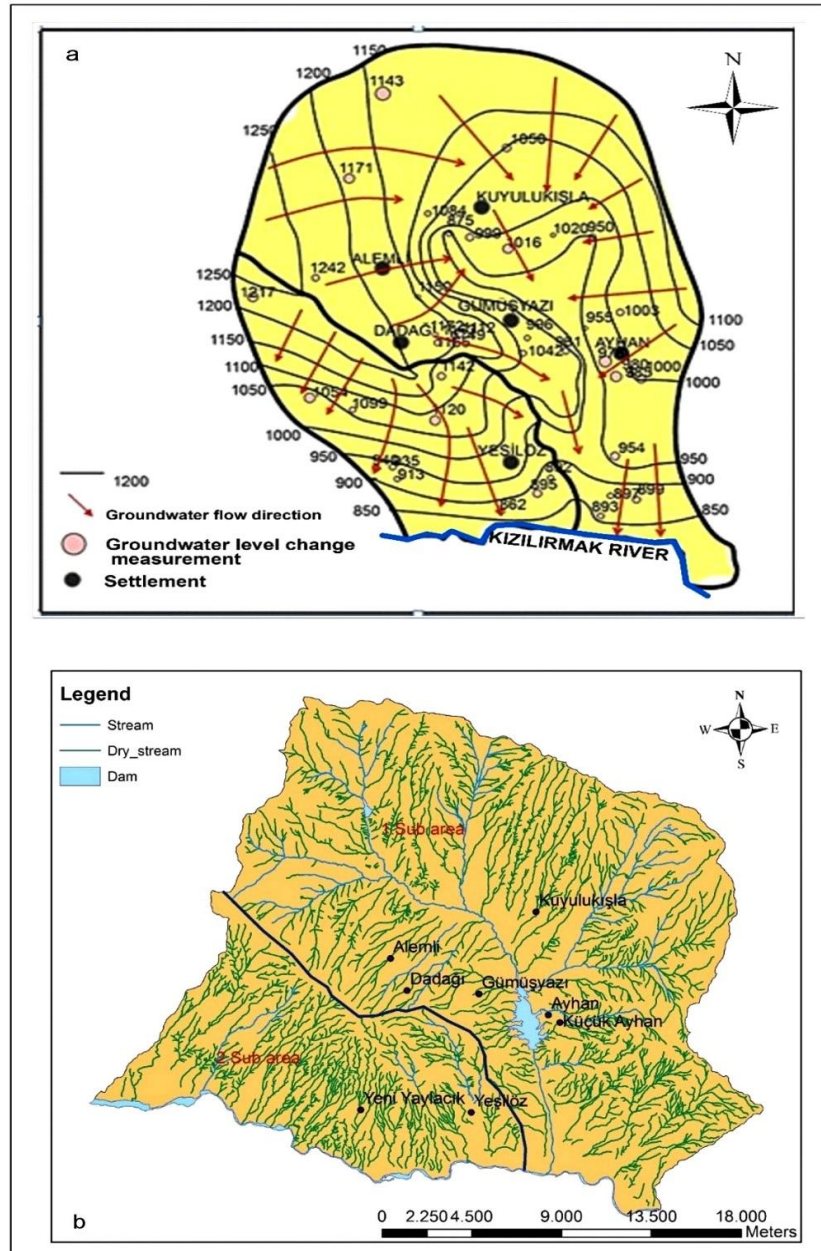
Fig. 4 *. (a) The isomorphic curves of the study area and the flow direction.*
(b) Study area sub-basin drainage network map.

Hydrogeochemical assessment of water resources

The water resources in the region are generally Ca, Mg-HCO$_3^-$ containing waters. In the study area, 10 samples (SMP) were collected in May, but it was observed that one (SMP4) of the springs dried up in September. The locations of the samples taken are shown on the map (Fig. 2). There is a significant decrease in the flow rates of other springs. Some of the samples taken belong to the wells.

Chemical properties of water resources

The results of the analyses of the main cations and anions of the water sources for the May 2019 rainy season are shown in Table 1. The analysis results for the September 2019 dry season are presented in Table 2.

Table 1 Chemical parameters (May 2019).

May.2019	Ca [mg/L]	Mg [mg/L]	Na [mg/L]	K [mg/L]	pH	Conductivity [μS/cm]	Hardness [mg CaCO₃/L]	Total Alkalinity [mg CaCO₃/L]	CO₃ [mg/L]	HCO₃ [mg/L]	Chloride [mg/L]
SMP1	225,7	101,3	99,2	9,782	7,76	2121	842	270	1,743	327,6	420,15
SMP2	99,05	21,44	28,06	7,690	7,5	683	290	320	1,138	389,2	13,10
SMP3	141,5	39,3	67,68	7,864	7,8	1179	470	275	1,945	333,5	128,27
SMP4	89,07	27,37	34,52	5,808	7,97	679	304	285	2,974	344,6	11,35
SMP5	101,5	21,38	29,12	2,991	7,47	664	316	315	1,046	383,2	9,99
SMP6	49,56	39,19	36,89	3,408	7,89	600	280	305	2,651	369,4	8,54
SMP7	45,84	36,2	28,91	1,263	8,09	536	248	290	3,978	349,7	4,65
SMP8	39,75	26,76	25,21	1,790	8,41	446	220	211,72	1,386	258,3	3,85
SMP9	58,74	46,21	47,84	4,863	7,87	741	320	375	3,114	454,3	10,12
SMP10	79,96	46,61	40,61	2,244	8,03	786	364	300	3,589	362,3	0

Ca: Calcium, Mg: Magnesium, Na: Sodium, K: Potassium, HCO₃: Bicarbonate, CO₃:Carbonate.

Table 2 Chemical parameters (September 2019).

Sep.2019	Ca [mg/L]	Mg [mg/L]	Na [mg/L]	K [mg/L]	pH	Conductivity [μS/cm]	Hardness [mg CaCO₃/L]	Total Alkalinity [mg CaCO₃/L]	CO₃ [mg/L]	HCO₃ [mg/L]	Chloride [mg/L]
SMP1	167,6	146,6	77,8	8,4	7,91	2014	833	250	2,274	302,6	374,00
SMP2	83,8	20,6	10,9	2,6	8,24	592	292	305	5,881	366	9,9134
SMP3	85,5	51,5	47,0	8,5	7,97	946	380	335	3,495	405,1	45,223
SMP5	207,8	83,2	43,1	5,1	7,55	1509	756	760	3,032	924,1	25,919
SMP6	38,3	63,6	25,2	4,6	8,31	605	266	310	6,693	371,2	13,546
SMP7	40,3	65,2	21,7	3,0	8,78	575	262	280	3,128	338,4	8,6331
SMP8	46,6	56,1	23,3	2,2	8,41	574	252	275	3,073	332,3	6,8753
SMP9	53,1	90,3	35,5	4,7	8,49	801	372	385	4,302	465,3	17,108
SMP10	70,7	90,1	34,1	2,4	8,44	826	390	300	3,352	362,5	6,3351

Ca: Calcium, Mg: Magnesium, Na: Sodium, K: Potassium, HCO₃: Bicarbonate, CO₃:Carbonate.

The results of the chemical analyses of the waters and in-situ measurements made in the field were graphed and interpreted. To investigate the hydrogeochemical properties of the water resources in the region, on-site measurements were made at all water points, samples (SMP) were collected for analysis, and the physical and chemical properties of the waters were determined.

The results of May period analyses show that pH values vary between 7.5 (SMP2) and 8.41 (SMP8); calcium (Ca) values vary between 39.75 mg/l (SMP8) and 225.7 mg/l (SMP1) and are concentrated south of the Ayhan shear zone. Magnesium (Mg) values vary between 21.44 mg/l (SMP2) and 101.3 mg/l (SMP1); potassium (K) values vary between 1.263 mg/l (SMP7) and 9.772 mg/l (SMP1) and increase in the southern part of the Ayhan shear zone where tectonic activity is also high (Table 2). Carbonate (CO_3) values vary between 1.046 mg/l (SMP5) and 3.978 mg/l (SMP7) and increase towards the north. Bicarbonate (HCO_3) values vary between 258.3 mg/l (SMP8) and 389.2 mg/l (SMP2), and chloride (Cl^-) values increase towards the south of the country, i.e. in the area of Tuzköy and Yüksekli formations representing the lake environment. Considering the dry season (September) data, Ca, Mg, and Na^+, K values of the springs are more intense in the south of the Ayhan shear zone. Carbonate (CO_3) values increase towards the north in the Ayhan shear zone. Chloride (Cl^-) values also increase towards the south of the country, i.e. in the area representing the lake environment. The ionic content of the water is given in the table below (Table 3). A diagram has been prepared. According to these values, the ion abundance diagram of the samples was prepared (Figure 5).

According to these chemical parameter tables, in terms of drinking water quality, the SMP1 sample is not suitable to be used as drinking water since Ca^{+2}, Mg^{+2}, $SO4^{-2}$, and Cl^-ions are above WHO (World Health Organization) and TS-266 (Turkish Standards) standard values. Other samples are suitable for drinking water use.

Table 3. *Ion content of water.*

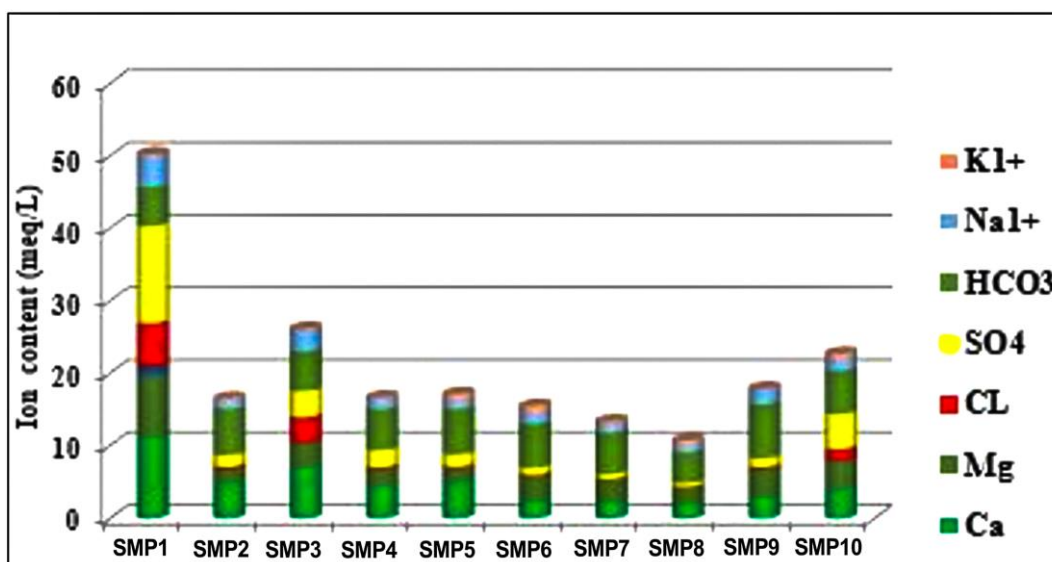|	Ca	Mg	Na^{1+}	K^{1+}	HCO$_3$	SO$_4$	Cl
Sample	mg/L	mg/L	mg/L	mg/L	mg/L	mg/L	mg/L
SMP1	11,29	8,44	4,31	0,25	5,37	13,39	6,21
SMP2	4,95	1,79	1,22	0,2	6,38	1,63	0,37
SMP3	7,08	3,28	2,94	0,2	5,47	3,59	3,61
SMP4	4,45	2,28	1,5	0,15	5,65	2,36	0,32
SMP5	5,08	1,78	1,27	0,8	6,28	1,66	0,28
SMP6	2,48	3,27	1,6	0,9	6,06	0,98	0,24
SMP7	2,29	3,02	1,26	0,3	5,73	0,66	0,13
SMP8	1,99	2,23	1,1	0,5	4,24	0,55	0,11
SMP9	2,94	3,85	2,08	0,12	7,45	1,2	0,29
SMP10	4	3,88	1,77	0,6	5,94	4,83	1,7

Fig. 5. Ion abundance diagram of the samples.

Cations and anions

Ca^{+2}: this ion must have mixed with the water as a result of washing the limestones with CO$_2$ water and, in volcanic areas, as a result of the dissolution of the Ca^{+2} ion in the silicate minerals such as anorthite, pyroxene, and amphibole (Table 3).

Mg^{+2}: This ion indicates that the surrounding ultramafic rocks (dolomite and gabbro) are related to water. Na^{+2}: may have entered the water by ion exchange due to the increased solubility of albites in volcanic rocks. Clay minerals cause Ca^{+2} to be replaced by Na^{+2}. SO$_4^{-2}$: This ion is enriched in gypsum, volcanic and atmospheric waters when it comes into contact with evaporites during water circulation. The HCO$_3^-$ ion in water is released by carbon dioxide gas and carbonate rocks.

According to the analysis results of water resources in the study area, Na$^+$+K$^+$ and minerals from clayey layers of the Tuzköy Formation and Yüksekli Formation, Ca^{+2} and Mg^{+2} from rocks of Tamadağ and Bozçaldağ Formations, Cl from evaporites and rain and snow water, as a result of the dissolution of travertines of Balkaya Formation and marbles of Bozçaldağ Formation, HCO$_3$ was dissolved at high rates and enriched in water resources.

Piper diagram

Water measurements taken in the area show different facies characteristics. The mix of these facies and waters can be determined using the Piper diagram. The Piper diagrams for the May 2019 and September 2019 sampling periods of the groundwaters in the study are shown in Figure 6a and Figure 6b, respectively.
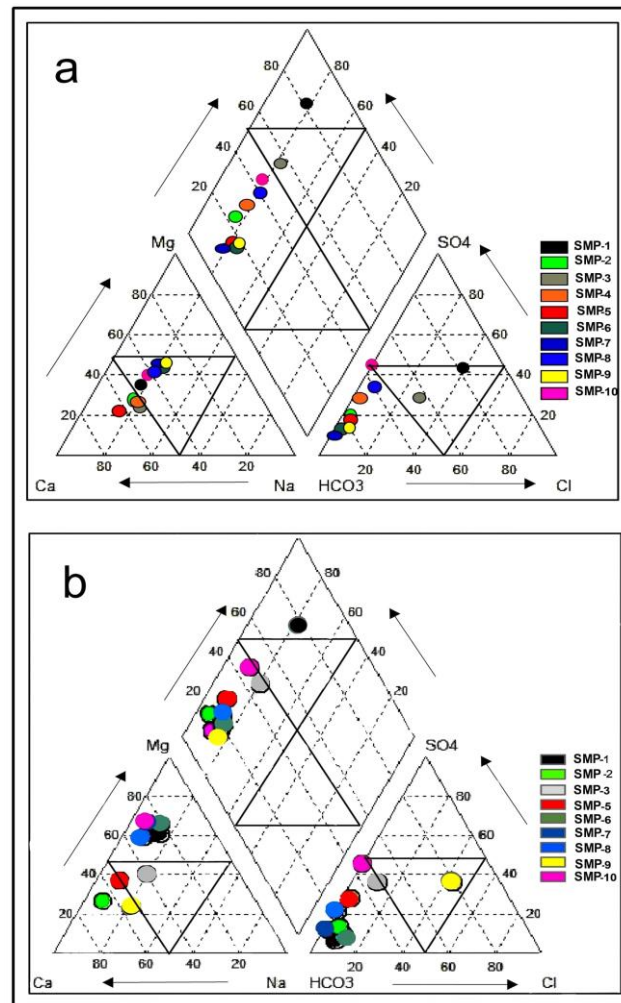

Fig. 6.   *(a) Piper diagram of the water samples around Gülşehir (Nevşehir) during the rainy period (May-2019)*
       (b) Piper diagram of dry period water samples in the vicinity of Gülşehir (Nevşehir) (September-2019)

In the May 2019 sampling period, all waters except SMP1 (with $CaSO_4$) and SMP3 (mixed waters) are Ca-$(HCO_3)_2$ type waters with high carbonate alkalinity and high hardness. The fact that these waters are Ca-$(HCO_3)_2$ facies indicates that they are fed by a carbonate aquifer. The clustering of waters in the same region on the Piper diagram indicates that they are fed by the same source or a similar aquifer.

When the analysis results of the September samples were examined on the Piper diagram, the Mg contents of samples SMP6, SMP7, SMP8, SMP9, and SMP10 increased. These waters are carbonate and dolomitic waters with high carbonate alkalinity and Ca-Mg$(HCO_3)_2$ waters with high hardness. The fact that these waters are Ca-Mg-HCO_3 facies indicates that they are fed by a carbonate aquifer with high dolomite content. The clustering of waters in the same region on the Piper diagram may indicate that the waters are fed by a related aquifer (Demircioğlu, 2021).

Heavy metal analysis, lithium values, and their relation to tectonic areas

In the study area, the heavy metal analyses in the water samples were examined (Table 4, 5). It was observed that the lithium values gave higher anomalies than the others (Fig. 7a, 7b). Lithium (Li) values range from 36.38 mg/l (SMP10) to 241.3 mg/l (SMP1). High lithium (Li) values are mostly found in the springs south of the survey area. Differences were observed according to the values taken from the structural areas, especially within the Ayhan shear zone. Lithium values are highest in the samples taken from the Kızılırmak graben area and the Tuzkoy and Yuksekli formations in this area (Figure 8).

In the Kızılırmak graben area (water samples taken from Tuzköy and Yüksekli formations), lithium levels were determined as 241.3 µg/L in (SMP1), 154.5 µg/L in (SMP2), 155.2 µg/L in (SMP3), 156.8 µg/L in (SMP4) and 155.6 µg/L in (SMP5). In the Ayhan shear zone area, 119.1 µg/L in (SMP6), 67.27 µg/L in (SMP7), 52.54 µg/L in (SMP8), 111.1 µg/L in (SMP9) and 36.38 µg/L in (SMP10) (Table 4).

Table 4. *May period analysis results.*

Sample no	Al [mg/L]	Li [mg/L]	Ni [mg/L]	Se [mg/L]	Zn [mg/L]
SMP-1	0,088	241,3	17,02	0,877	55,01
SMP-2	0	154,5	5,664	1,071	34,76
SMP-3	0	155,2	12,55	0,397	230,9
SMP-4	0	156,8	6,911	1,267	20,25
SMP-5	0	155,6	6,015	0,726	137,7
SMP-6	0	219,1	8,984	2,939	1,12
SMP-7	0	67,27	7,694	0,606	1,24
SMP-8	0	52,54	6,807	0,58	1,36
SMP-9	0	211,1	12,89	1,389	1,24
SMP-10	1,176	36,38	11,52	0,613	1,54

In the Kızılırmak graben area, lithium levels in the samples taken in September were measured as 184.8 µg/L in (SMP1), 50.96 µg/L in (SMP2), 121.5 µg/L in (SMP3) and 340.9 µg/L in (SMP5). In the Ayhan shear zone area, 129.4 µg/L in (SMP6), (SMP7) 65.62 µg/L, 45.87 µg/L in (SMP8), 119.9 µg/L in (SMP9), and 36.82 µg/L in (SMP10) (Table 5).

Table 5. *September period analysis results.*

Sample No	Al [mg/L]	Li [mg/L]	Ni [mg/L]	Se [mg/L]	Zn [mg/L]
SMP1	14,22	184,8	63,04	15,95	472,8
SMP2	14,32	50,96	26,86	19,2	157,9
SMP3	15,61	121,5	38,4	20,39	35
SMP5	18,76	340,9	49,32	30,57	118,2
SMP6	11,16	169,4	40,13		74,37
SMP7	9,293	65,62	41,21	19,66	0
SMP8	6,944	45,87	36,6	19,23	19,26
SMP9	6,511	139,9	46,75	23,73	0
SMP10	11,13	36,82	44,4	19,71	4,35

The determined lithium and other heavy metal values are shown in the diagrams (Figure 7a, 7b).
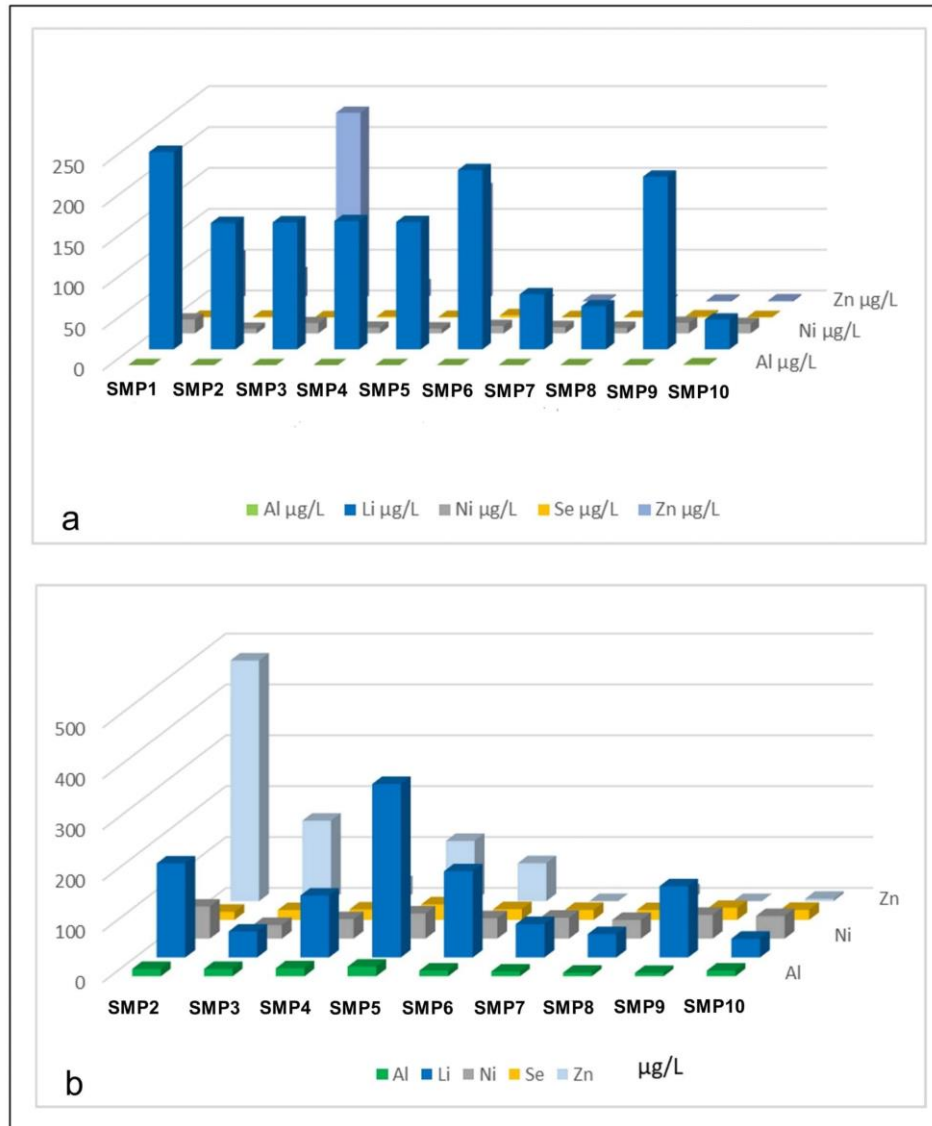
Fig. 7. (a) Graph of heavy metal and lithium values for May.

(b) Graph of heavy metal and lithium values for September.

The high lithium values in the study area are probably due to the combination of salt layers formed in the residual lakes of marine origin and young volcanic activity. Thick salt layers are observed in the area (Figure 8).
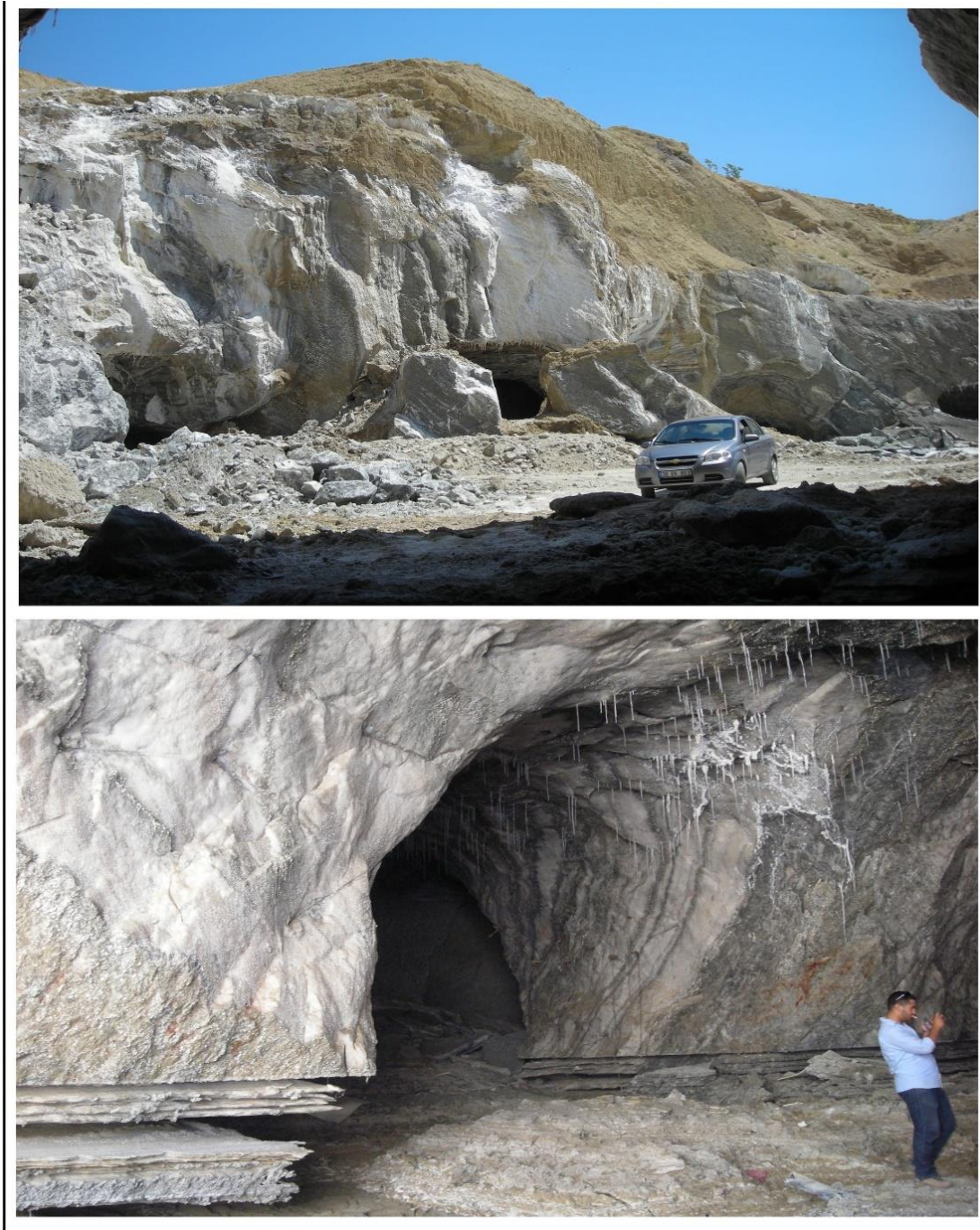
Fig. 8. Tuzköy formation and salt cave.

IDW and Kernel diagrams for lithium values

The values of lithium obtained from the water analysis were evaluated in IDW (Inverse Distance Weighting) and Kernel plots, and their diagrams were prepared using Arc-GIS software (Figs. 9, 10, 11).
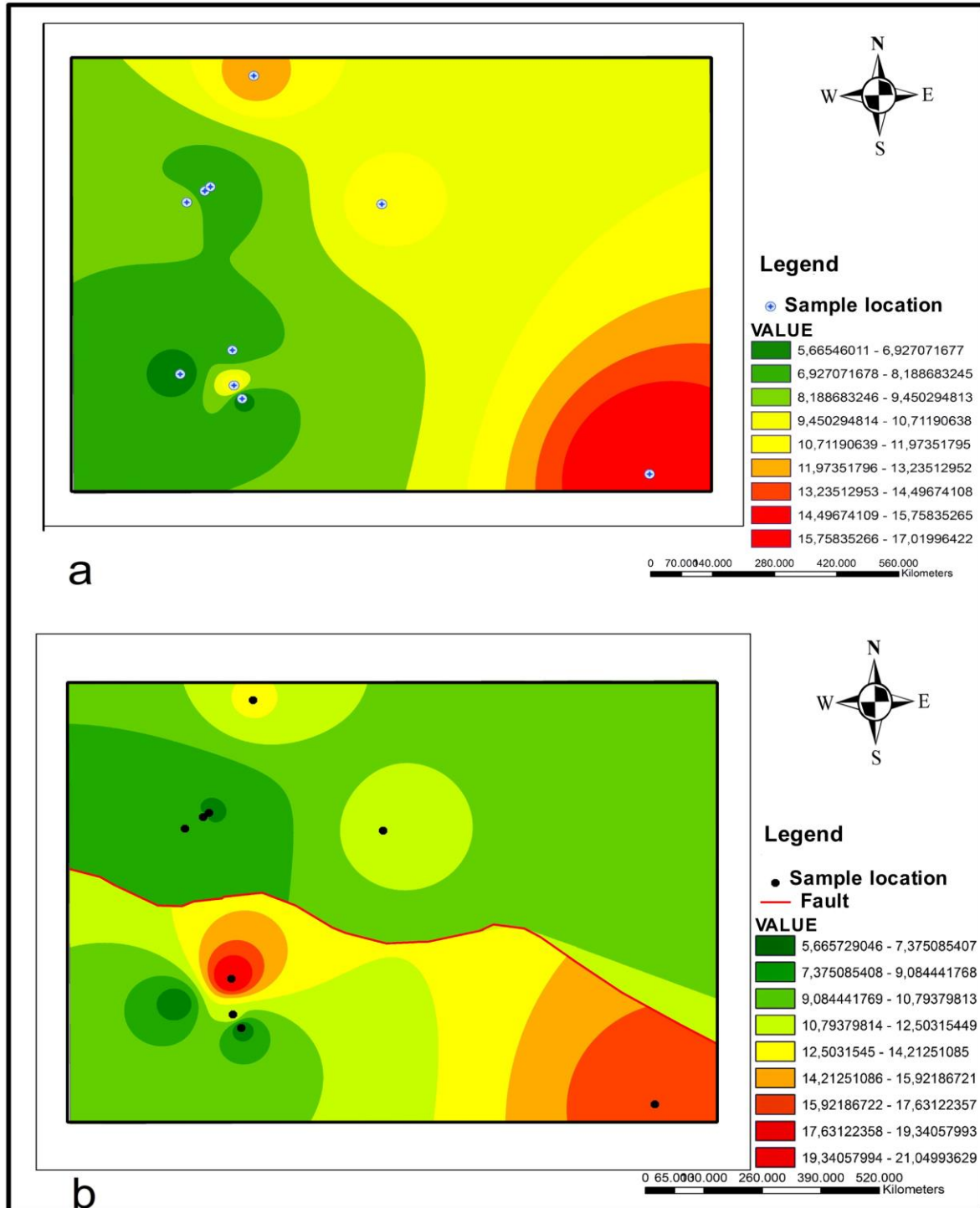
Fig. 9. IDW diagrams were prepared according to lithium (May) values in the area. (a) no-fault (b) with fault).
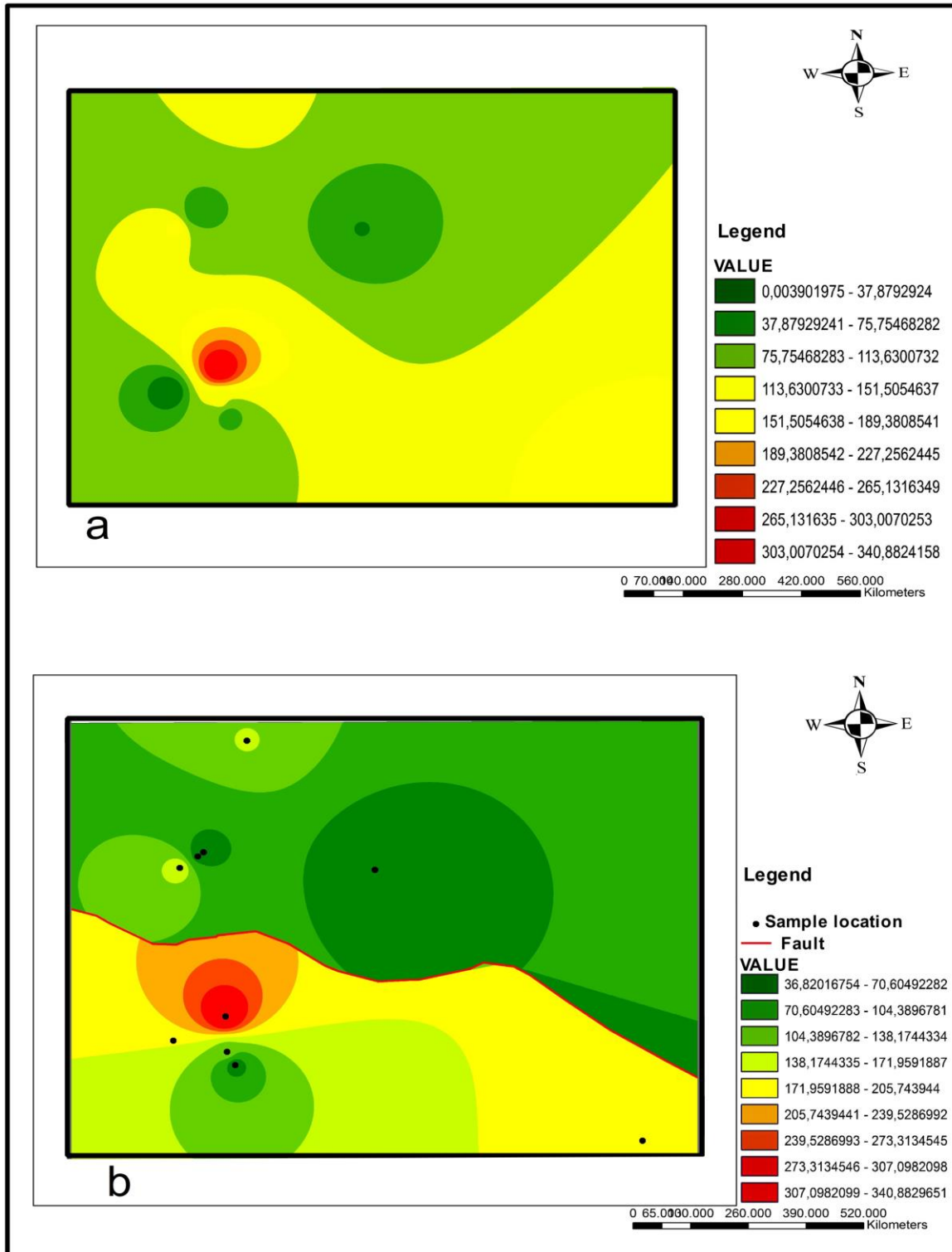
Fig. 10. IDW diagrams prepared according to lithium (September) values in the area (a) no-fault (b)with fault).

In addition, their relationship with structural areas was evaluated. These plots are based on the estimated density calculation, which is inversely proportional to the source distances. Kernel diagrams for lithium values were also generated (Fig. 11). It is believed that the IDW plots give more accurate results. When the plots are examined, it can be seen that the IDW plots give narrower and more accurate areas.
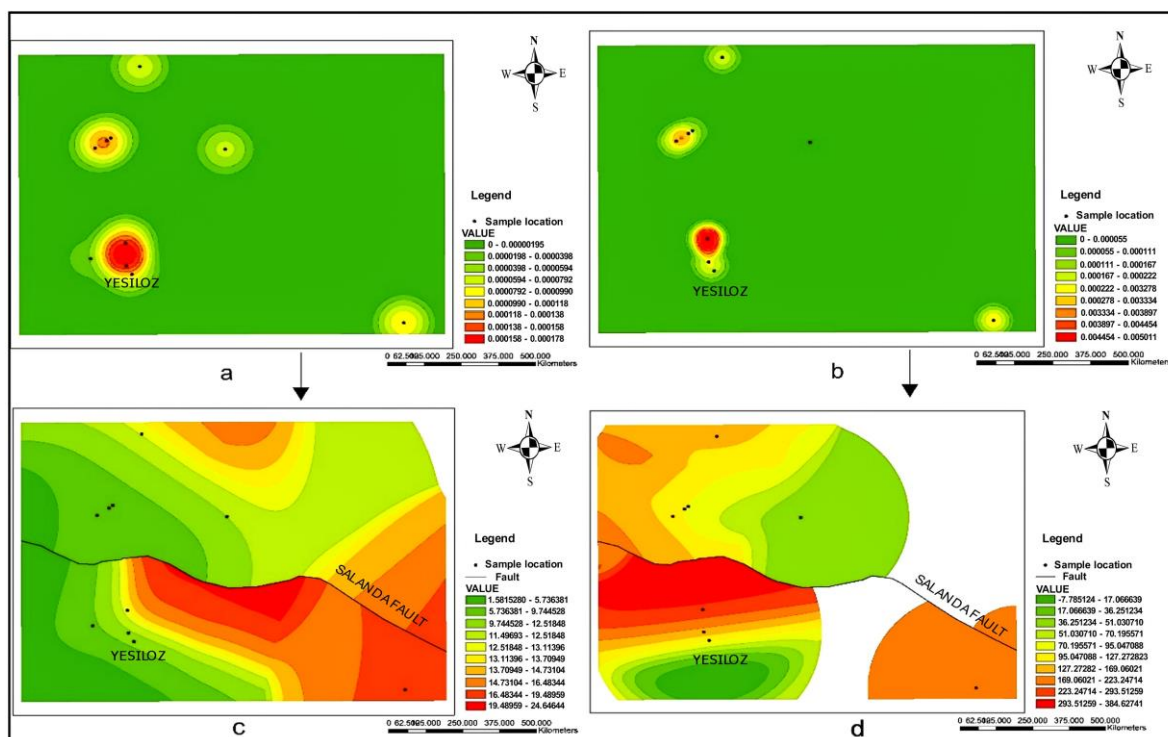
Fig. 11. Kernel diagrams, no-fault (a, b) and with the fault (c-d), (a-c: may, b-d: September).

This graph shows the relationship between structural area, fault (Salanda Fault), and lithium ratios. Lithium values are highest in the area near the Salanda fault. In the Ayhan shear zone, there is one sample (SMP9) with high lithium values. Considering that these areas are marine and saline lake environments, both lithological and structural features appear to have influenced the lithium rates. The lithium content in the water samples taken from the Kızılırmak graben, where the Tuzköy and Yuksekli formations are located, gives the highest values. The origin of lithium in the study area can be determined more precisely by studying and analyzing other areas.

Conclusions

Lithium values are highest in the region close to the Salanda fault, i.e., in the sample taken from the Kızılırmak graben (SMP5). Only one sample (SMP9) with high lithium values is in the Ayhan shear zone. Considering that these areas are marine and saline lake environments where volcanic rocks such as tuff and tuffite also occur, it is evident that both lithological and structural features affect lithium formation and ratios. The lithium content in the water samples taken from the Kızılırmak graben, where Tuzköy and Yüksekli formations, which are composed of volcano-sedimentary units, give the highest values. An attempt was made to determine the hydrogeochemical properties of the rocks in the study area and the variation in lithium values. According to the results, all waters in the area, except SMP1 (containing $CaSO_4$) and SMP3 (mixed waters), are $Ca-(HCO_3)_2$ type waters with high carbonate alkalinity and high hardness. The $Ca-(HCO_3)_2$ facies of these waters indicate that they are recharged from a carbonate aquifer. Lithium (Li) values vary between 36.38 mg/l (SMP10) and 241.3 mg/l (SMP1). High lithium (Li) values are generally higher in the area within the Kızılırmak graben. In the study area, lithium levels in the water samples taken in May were determined as 241.3 µg/L, 154.5 µg/L, 155.2 µg/L, 156.8 µg/L and 155.6 µg/L in the graben area. In the Ayhan shear zone area, 119.1 µg/L, 67.27 µg/L, 52.54 µg/L, 111.1 µg/L, and 36.38 µg/L were measured. In the samples taken in September, lithium levels were measured as 184.8 µg/L, 50.96 µg/L, 121.5 µg/L, and 340.9 µg/L in the graben area. In the Ayhan shear zone area, 129.4 µg/L, 65.62 µg/L, 45.87 µg/L, 119.9 µg/L, and 36.82 µg/L were measured. The high values in this area are due to the saline Tuzköy and Yuksekli formations, which are the former salt lake area.

Due to the uplift of the marine region after the Middle Eocene, units belonging to the Late Miocene Tuzköy and Yuksekli formations were formed in the region, which was transformed into a lakeshore environment. Salt minerals such as halite formed in these formations also affected the groundwater and increased the salinity. Lithium-bearing minerals are generally abundant in salt lake environments. This is supported by the fact that most of the lithium mines in operation today are located in former salt lake environments. The geological-tectonic evolution of the region has also influenced water chemistry.

References

Atabey, E., Tarhan, N. Yusufoğlu, H. and Canpolat, M., (1988). Hacıbektaş, Gülşehir, Kalaba (Nevşehir) Himmetdede (Kayseri) arasının jeolojisi. *M.T.A. Rapor No: 8523, (Unpublished).*

Aydar, E., Schmitt, A., Çubukçu, E., Akın, L., Ersoy, O., Şen, E., Duncan, R., and Atıcı, G., (2012). Correlation of ignimbrites in the Central Anatolian volcanic province using zircon and plagioclase ages and zircon composition. *Journal of Volcanology and Geothermal Research.* 214, 83–97p. *https://doi.org/10.1016/j.jvolgeores.2011.11.005*

Aydın, N., (1984). Orta Anadolu masifinin Gümüşkent (Nevşehir) dolayında jeolojik-petrografik incelemeler. Doktora tezi, Ank.Ün. Fen Fak., 400 p., Ankara.

Batum, İ., (1978). Göllüdağ ve Acıgöl volkanitlerinin jeokimyası ve petrolojisi. *Yerbilimleri. 3–4, 70–88.*

Belova, T. P., (2017). Experimental studies in the sorptive extraction of boron and lithium from thermal waters. *Journal of Volcanology and Seismology, 11(2), 136–142. https://doi.org/10.1134/S0742046317020026*

Demircioğlu, İ., (2021). Gülşehir bölgesindeki su kaynaklarının hidrojeolojik incelemesi. Yüksek lisans tezi, Aksaray Ü. Fen Bilimleri Enstitüsü, Aksaray, 84p.

Demircioğlu, R., (2014). Gülşehir-Özkonak (Nevşehir) çevresinde Kırşehir Masifi ve örtü birimlerinin jeolojisi ve yapısal özellikleri, Doktora Tezi, S.Ü. Fen Bilimleri Enstitüsü, Konya, 232 p.

Demircioğlu, R., and Eren, Y., (2021). Ayhan kayma zonunun (Avanos-Nevşehir, Orta Anadolu) yapısal özellikleri. *Türkiye. 73, Jeoloji Kurultayı, Ankara, 180–181.*

Doğan, U., Koçyigit, A. and Wijbrans, J., (2009). Kızılırmak nehrinin evrimsel tarihi, Kapadokya kesimi: Iç Anadolu bölgesi'nde neotektonik rejimin baslangici için bir çikarsama*, Türkiye. 62. Jeoloji Kurultayı, Ankara, 806–807.*

Ercan, T., Akbaşlı, A., Yıldırım, T., Fişekçi, A., Selvi, Y., Ölmez, M., and Can, B., (1991). Acıgöl (Nevşehir) yöresindeki Senezoyik yaşlı volkanik kayaçların petrolojisi., *MTA Dergisi, 113, 31–44.*

Godfrey, L., and Álvarez-Amado, F. (2020). Volcanic and saline lithium inputs to the Salar de Atacama. *Minerals,* 10*(2), 201.*

Göncüoğlu, C., Yalınız, K., Kuşçu, I., Köksal, S., and Dirik, K. (1993). Orta Anadolu Masifinin orta bölümünün jeolojisi, Bolum 3: Orta Kızılırmak tersiyer baseninin jeolojik evrimi. *T.P.A.O. Rapor No: 3313.*

Huang, Y.; and Wang, R. (2018). An efficient lithium-ion imprinted adsorbent using multi-wall carbon nanotubes as support to recover lithium from water. *Journal of Cleaner Production, 205, 201–209.* *https://doi.org/10.1016/j.jclepro.2018.09.076*

Huang, Y., and Wang, R. (2019). Green recovery of lithium from water by a smart imprinted adsorbent with photo-controlled and selective properties. *Chemical Engineering Journal, 378, 122084.* *https://doi.org/10.1016/j.cej.2019.122084*

Ighalo, J.O.; Amaku, J.F.; Olisah, C.; Adeola, A.O.; Iwuozor, K.O.; Akpomie, K.G., & Oyedotun, K.O. (2022). The utilization of adsorption as a resource recovery technique for lithium in geothermal water. *Journal of Molecular Liquids, 120107. https://doi.org/10.1016/j.molliq.2022.120107*

Kaunda, R.B. (2020). Potential environmental impacts of lithium mining. *Journal of energy & natural resources law, 38(3), 237–244. https://doi.org/10.1080/02646811.2020.1754596*

Kavanagh, L.; Keohane, J.; Cleary, J.; Garcia, Cabellos, G., & Lloyd, A. (2017). Lithium in the natural waters of the South East of Ireland. *International Journal of Environmental Research and Public Health, 14(6), 561.* *https://doi.org/10.3390/ijerph14060561*

Ketin, İ., (1966). Tectonic units of Anatolia. *Mineral Res. Explor. Bull, 66, 23–34.*

Kim, N., Su, X., and Kim, C. (2021). Electrochemical lithium recovery system through the simultaneous lithium enrichment via a sustainable redox reaction. *Chemical Engineering Journal, 420, 127715.*

Köksal, S., and Göncüoglu, M.C. (1997). İdiş Dağı-Avanos alanının jeolojisi (Nevşehir-Orta Anadolu). *Maden Tetkik ve Arama Dergisi, s: 119, s. 73–89.*

Kuşcu, I. (2001). Geochemistry and mineralogy of the skarns in the Celebi district, Kirikkale, Turkey. *Turkish Journal of Earth Sciences, 10. 121-132. https://journals.tubitak.gov.tr/earth/vol10/iss3/3*

Li, B., Wu, J., and Li, L. (2021). Speciation and correlation of boron and lithium in surficial sediments of the eastern and western Taijinar Salt Lake. *Environmental Earth Sciences,* 80*(10), 382.*

Li, Y. L., Miao, W. L., He, M. Y., Li, C. Z., Gu, H. E., and Zhang, X. Y. (2023). Origin of lithium-rich salt lakes on the western Kunlun Mountains of the Tibetan Plateau: Evidence from hydrogeochemistry and lithium isotopes. *Ore Geology Reviews,* 155*, 105356. https://doi.org/10.1016/j.oregeorev.2023.105356*

Liu, W., and Agusdinata, D.B. (2020). Interdependencies of lithium mining and communities sustainability in Salar de Atacama, Chile. *Journal of Cleaner Production, 260, 120838.* *https://doi.org/10.1016/j.jclepro.2020.120838*

Okay, A.İ., and Tüysüz, O. (1999). Tethyan sutures of northern Turkey. In: Durand, B. ,Jolivet, L., Horváth, F., Séranne, M. (Eds.), The Mediterranean Basins: Tertiary extension within the alpine orogen. *Geological Society*, London, Special Publications*, 156, 475–515. https://doi.org/10.1144/GSL.SP.1999.156.01.22*

Özdemir, A., Palabiyik, Y., Karataş, A., and Sahinoglu, A. (2022). Mature petroleum hydrocarbon contamination in surface and subsurface waters of Kızılırmak Graben (Central Anatolia), Turkey): Geochemical evidence for a working petroleum system associated with a possible salt diapir. *Turkish Journal of Engineering. 6(1), 1–15.* https://doi.org/10.31127/tuje.747379

Seymen, İ. (1982). Kaman dolayında Kırşehir masifi'nin jeolojisi, Doçentlik Tezi, Î.T.Ü. Maden Fakültesi, İstanbul,164 p.

Sulistiyono, E., Harjanto, S., and Lalasari, L.H. (2022). Separation of magnesium and lithium from brine water and bittern using sodium silicate precipitation agent. *Resources, 11(10), 89–99.* https://doi.org/10.3390/resources11100089

TSE 266 (2005). Turkish Standards, Waters for Human Consumption.

Wang, H., Cui, J., Li, M., Guo, Y., Deng, T., and Yu, X., (2020). Selective recovery of lithium from geothermal water by EGDE cross–linked spherical CTS/LMO. *Chemical Engineering Journal, 389, 124410.* https://doi.org/10.1016/j.cej.2020.124410

WHO (2011) Guidelines for drinking-water quality, World Health Organization.

Zante, G., Boltoeva, M., Masmoudi, A., Barillon, R., and Trebouet, D. (2019). Lithium extraction from complex aqueous solutions using supported ionic liquid membranes. *Journal of Membrane Science, 580, 62–76.* https://doi.org/10.1016/j.memsci.2019.03.013

Zhang, Y., Sun, W., Xu, R., Wang, L., and Tang, H. (2021). Lithium extraction from water lithium resources through green electrochemical-battery approaches: A comprehensive review. *Journal of Cleaner Production, 285, 1249.* https://doi.org/10.1016/j.jclepro.2020.124905